RUBIDIUM AND LEAD ABUNDANCES IN GIANT STARS
OF THE GLOBULAR CLUSTERS M13 AND NGC 6752[1]

DAVID YONG

Department of Physics and Astronomy, University of North Carolina,
Chapel Hill, NC 27599-3255; yong@physics.unc.edu

WAKO AOKI

National Astronomical Observatory, Mitaka, 181-8588 Tokyo, Japan; aoki.wako@nao.ac.jp

DAVID L. LAMBERT

Department of Astronomy, University of Texas, Austin, TX 78712; dll@astro.as.utexas.edu

AND

DIANE B. PAULSON

NASA Goddard Space Flight Center, Code 693.0, Greenbelt, MD 20771; diane.b.paulson@gsfc.nasa.gov

ABSTRACT

We present measurements of the neutron-capture elements Rb and Pb in five giant stars of the globular cluster NGC 6752 and Pb measurements in four giants of the globular cluster M13. The abundances were derived by comparing synthetic spectra with high-resolution, high signal-to-noise ratio spectra obtained using HDS on the Subaru telescope and MIKE on the Magellan telescope. The program stars span the range of the O–Al abundance variation. In NGC 6752, the mean abundances are $[\mathrm{Rb/Fe}] = -0.17 \pm 0.06$ ($\sigma = 0.14$), $[\mathrm{Rb/Zr}] = -0.12 \pm 0.06$ ($\sigma = 0.13$), and $[\mathrm{Pb/Fe}] = -0.17 \pm 0.04$ ($\sigma = 0.08$). In M13 the mean abundance is $[\mathrm{Pb/Fe}] = -0.28 \pm 0.03$ ($\sigma = 0.06$). Within the measurement uncertainties, we find no evidence for star-to-star variation for either Rb or Pb within these clusters. None of the abundance ratios $[\mathrm{Rb/Fe}]$, $[\mathrm{Rb/Zr}]$, or $[\mathrm{Pb/Fe}]$ are correlated with the Al abundance. NGC 6752 may have slightly lower abundances of $[\mathrm{Rb/Fe}]$ and $[\mathrm{Rb/Zr}]$ compared to the small sample of field stars at the same metallicity. For M13 and NGC 6752 the Pb abundances are in accord with predictions from a Galactic chemical evolution model. If metal-poor intermediate-mass asymptotic giant branch stars did produce the globular cluster abundance anomalies, then such stars do not synthesize significant quantities of Rb or Pb. Alternatively, if such stars do synthesize large amounts of Rb or Pb, then they are not responsible for the abundance anomalies seen in globular clusters.

Subject headings: Galaxy: abundances — globular clusters: individual (M13, NGC 6752) — stars: abundances

Online material: color figures

1. INTRODUCTION

Globular clusters are ideal laboratories for testing the predictions of stellar evolution theory (e.g., Renzini & Fusi Pecci 1988), since the individual stars are believed to be monometallic, coeval, and at the same distance. In a given globular cluster (excluding ω Cen), spectroscopic observations of individual stars have confirmed that members have uniform compositions, at least for the Fe-peak elements (e.g., see review by Gratton et al. 2004 and references therein). However, it has been known for many years now that globular clusters exhibit star-to-star abundance variations for the light elements C, N, O, Na, Mg, and Al (e.g., see review by Kraft 1994). Specifically, the abundances of C and O are low when N is high and anticorrelations are found between O and Na, as well as Mg and Al. Recently, variations in the abundance of fluorine have been discovered in giants in M4 where the amplitude of the dispersion exceeds that of O (Smith et al. 2005).

It is generally assumed that the light-element variations arise from proton-capture reactions (CNO cycle, Ne-Na chain, and Mg-Al chain), although the specific nucleosynthetic site(s) remain elusive. One possibility for the origin of the star-to-star abundance variations is deep mixing and internal nucleosynthesis within the observed stars. Evidence for this "evolutionary scenario" includes C and N abundances (Suntzeff & Smith 1991) that vary with location on the red giant branch (RGB). Extensive mixing down to very hot layers is necessary to change the surface composition of Na, Mg, and Al. Such mixing is not predicted by standard models, and the proposed mechanisms include meridional circulation (Sweigart & Mengel 1979), turbulent diffusion (Charbonnel 1995), and hydrogen-burning shell flashes (Fujimoto et al. 1999; Aikawa et al. 2001, 2004). An alternative possibility is pollution from intermediate-mass asymptotic giant branch stars (IM-AGBs), first suggested by Cottrell & Da Costa (1981) to explain the Na and Al enhancements observed in CN-strong stars in NGC 6752. In IM-AGBs, hydrogen burning at the base of the convective envelope, so-called hot bottom burning (HBB), can produce the observed C to Al abundance patterns. Either the ejecta from IM-AGBs pollute the protocluster gas from which the present cluster members form, or the ejecta are accreted by present cluster members. The strongest evidence for this "primordial scenario" has come from observations of main-sequence stars in which abundance variations of O, Na, Mg, and Al have been found (Gratton et al. 2001; Ramírez & Cohen 2003; Cohen &

Meléndez 2005). In these unevolved stars, the internal temperatures are too low to run the Ne-Na or Mg-Al chains, which therefore precludes internal mixing as a viable explanation for the star-to-star composition differences.

In M4, Smith et al. (2005) found that F varied from star to star and that the F abundance was correlated with O and anticorrelated with Na and Al. Since destruction of F is expected to take place during HBB in IM-AGBs (Lattanzio et al. 2004), the observed dispersion of F is in qualitative agreement with IM-AGBs being responsible for the globular cluster abundance anomalies. However, a quantitative test involving recent yields for AGB stars combined with a standard initial mass function showed that the observed abundance variations cannot be reproduced via pollution from AGB stars (Fenner et al. 2004). Denissenkov & Herwig (2003) and Denissenkov & Weiss (2004) also find flaws in the AGB pollution scenario based on calculated yields from AGB models. Ventura & D'Antona (2005) caution that theoretical yields from AGB models are critically dependent on the assumed mass-loss rates and treatment of convection such that the predictive power of the current AGB models is diminished. That there is still no satisfactory explanation for the star-to-star abundance variations seen in every well-studied Galactic globular cluster would suggest that our understanding of globular cluster chemical evolution and stellar nucleosynthesis is incomplete.

Two neutron-capture elements, rubidium and lead, may offer further clues regarding the processes that gave rise to the star-to-star abundance variations and possibly the formation of globular clusters. Rb has two stable isotopes, ^{85}Rb and ^{87}Rb. While the solar abundance of Rb is due to 50% s-process and 50% r-process (Burris et al. 2000), the abundance of Rb relative to nearby elements such as Sr, Y, and Zr offers an insight into the neutron density at the site of the s-process and therefore the mass of the AGB star due to the 10.7 yr half-life of ^{85}Kr (e.g., Tomkin & Lambert 1983, 1999; Lambert et al. 1995; Busso et al. 1999; Abia et al. 2001). Along the s-process path, Rb is preceded by Kr. The path enters at ^{80}Kr and exits at either ^{85}Kr or ^{87}Kr, with ^{85}Kr providing the branching point. At low neutron densities ($N_n \leq 1 \times 10^8$ cm^{-3}), ^{85}Kr β-decays to the stable isotope ^{85}Rb. At high neutron densities, ^{85}Kr will capture neutrons to form ^{86}Kr and then ^{87}Kr, which β-decays to ^{87}Rb (effectively stable, with a half-life of 4.7×10^{10} yr). Clearly, the isotopic mix of Rb depends on the neutron density. Unfortunately, stellar Rb isotope ratios cannot be measured (Lambert & Luck 1976). In the presence of a steady flow along the s-process path, the density of a nuclide satisfies the condition $\sigma_i N_i \simeq$ constant, where σ_i and N_i are the cross section and abundance of nuclide i, respectively. The neutron-capture cross sections differ by a factor of 10 between the two Rb isotopes ($\sigma_{87} = \sigma_{85}/10$). The ^{85}Kr branch does not affect the Zr abundances, since the low and high neutron density s-process paths converge at Sr. Therefore, in a high neutron density environment such as the helium intershell during a thermal pulse in IM-AGBs, the Rb abundance may increase by a factor of 10 relative to nearby s-process elements such as Sr, Y, and Zr. In reality, the situation is slightly more complex, since neutron capture on ^{84}Kr leads to the ground state of ^{85}Kr, as well as a short-lived isomeric state that decays to either the ^{85}Kr ground state or ^{85}Rb (see Beer & Macklin 1989 for more details). IM-AGBs of solar metallicity are expected to have a high neutron density, with ^{22}Ne (α, n) ^{25}Mg providing the neutron source. [Low-mass AGB stars, whose neutron source is ^{13}C (α, n) ^{16}O, provide a lower neutron density.] For metal-poor or zero-metallicity IM-AGBs, Busso et al. (2001) suggest that such stars do run the s-process, although the details are model dependent. Nevertheless, the Rb abundance relative to Sr, Y, and Zr (which are not affected by the ^{85}Kr branch) is a potential diagnostic of the s-process site and may offer an additional insight into the role of IM-AGBs in the chemical evolution of globular clusters.

The isotopes of Pb, along with bismuth, comprise the last stable nuclei along the s-process path. In low-mass AGB stars, the neutron source is provided by ^{13}C, whereas in IM-AGBs, ^{22}Ne provides the neutron source, with the division occurring at roughly 4 $M_\odot$. In low-mass AGB stars and IM-AGBs of low metallicity, overabundances of Pb and Bi may be expected if the neutron supply per seed exceeds a certain value (e.g., Goriely & Mowlavi 2000; Travaglio et al. 2001; Busso et al. 2001). Goriely & Siess (2001) suggest that for AGB stars with $Z < 0.001$, the available neutrons per seed nucleus is greater than the number required to produce Pb and Bi. Travaglio et al. (2001) suggest that metal-poor IM-AGBs play only a minor role in the production of Pb, although for their 5 $M_\odot$ model, the Pb yields do not change between [Fe/H] $= -1.3$ and solar. Herwig (2004) suggests that metal-poor IM-AGBs efficiently activate the ^{22}Ne neutron source, although quantitative s-process yields are not presented. Busso et al. (2001) predict high yields of Pb from metal-poor IM-AGBs. The ratio of Pb/La and Pb/Ba can be used to probe the nature of the s-process in metal-poor AGB stars (Gallino et al. 1998; Goriely & Mowlavi 2000). Numerous observational studies have found considerable overabundances of Pb in stars that exhibit large s- and/or r-process enhancements (e.g., Cowan et al. 1996; Sneden et al. 2000; Aoki et al. 2000, 2001, 2002; Van Eck et al. 2001, 2003; Johnson & Bolte 2002; Lucatello et al. 2003; Sivarani et al. 2004; Ivans et al. 2005 and references therein). If the globular cluster star-to-star abundance variations are due to pollution from metal-poor IM-AGBs, we can expect large overabundances of Pb and a dispersion in Pb abundances despite the absence of variations and excesses in other s-process elements.

In this paper, we present measurements of Rb and Pb in the globular cluster NGC 6752, as well as measurements of Pb in the globular cluster M13. While Rb has been measured in two globular clusters, ω Cen (Smith et al. 2000) and NGC 3201 (Gonzalez & Wallerstein 1998), as far as we are aware these are the first measurements of Pb in a globular cluster. We chose the globular clusters M13 and NGC 6752 because they exhibit the largest amplitude for the Al variation of all the well-studied Galactic globular clusters and therefore offer the best opportunity to find abundance variations for Rb and Pb. Previous studies of M13 include Cohen (1978) and Peterson (1980), who found large Na variations; Shetrone (1996a, 1996b), who showed that the Mg isotope ratios were not constant; and Cohen & Meléndez (2005), who discovered abundance variations in unevolved stars; as well as analyses by Kraft et al. (1992, 1997), Pilachowski et al. (1996), and Sneden et al. (2004b). Previous studies of NGC 6752 include Cottrell & Da Costa (1981), who discovered the Na and Al enhancements; Suntzeff & Smith (1991), who found C and N to systematically vary according to evolutionary status; Gratton et al. (2001) and Grundahl et al. (2002), who discovered O−Al variations in unevolved stars; Yong et al. (2003a, hereafter Y03), who found variations in Mg isotope ratios; Yong et al. (2005, hereafter Y05), who presented evidence for slight abundance variations of Si, Y, Zr, and Ba; and Pasquini et al. (2005), who measured Li in main-sequence stars.

2. OBSERVATIONS AND DATA REDUCTION

The list of candidates included five giants in NGC 6752 previously studied in Y03 and Y05, four giants in M13 previously studied by Shetrone (1996a, 1996b), and the comparison star HD 141531, a giant whose evolutionary status and stellar parameters

TABLE 1
Exposure Times and Stellar Parameters

Star	Telescope	Exposure Time (minutes)	S/N (pixel^{-1}) 4050 Å	S/N (pixel^{-1}) 7800 Å	$T_{\rm eff}$ (K)	log g	ξ_t (km s^{-1})	[Fe/H]
M13 L598	Subaru	60	39	. . .	3900	0.00	2.25	−1.56
M13 L629	Subaru	50	37	. . .	3950	0.20	2.25	−1.63
M13 L70[a]	Subaru	60	39	. . .	3950	0.30	2.25	−1.59
M13 L973[b]	Subaru	64	36	. . .	3920	0.30	2.35	−1.61
NGC 6752 B702....................	Magellan	20	42	197	4050	0.50	2.10	−1.58
NGC 6752 B708....................	Magellan	50	55	402	4050	0.25	2.20	−1.63
NGC 6752 PD1	Magellan	26	47	197	3928	0.26	2.70	−1.62
NGC 6752 B1630..................	Magellan	27	44	247	3900	0.24	2.70	−1.60
NGC 6752 B3589..................	Magellan	21	46	240	3894	0.33	2.50	−1.59
HD 141531	Subaru	10	85	. . .	4273	0.80	1.90	−1.72

[a] Alternative name II-67.
[b] Alternative name I-48.

are comparable to the cluster giants. Although we were restricted to the brightest giants, the globular cluster stars were deliberately selected to span a large range of the star-to-star abundance variations. Table 1 contains the list of targets observed using either the Subaru or Magellan telescope.

Observations of the M13 giants and the comparison field star HD 141531 were obtained with the Subaru Telescope using the High Dispersion Spectrograph (HDS; Noguchi et al. 2002) on 2004 June 1. A 0″.4 slit was used, providing a resolving power of 90,000 per 4 pixel resolution element with wavelength coverage from 4000 to 6700 Å. For the Subaru data, one-dimensional wavelength-calibrated normalized spectra were produced in the standard way using the IRAF[2] package of programs.

Observations of the NGC 6752 giants were obtained with the Magellan Telescope using the Magellan Inamori Kyocera Echelle spectrograph (MIKE; Bernstein et al. 2003) on 2004 April 3–5.
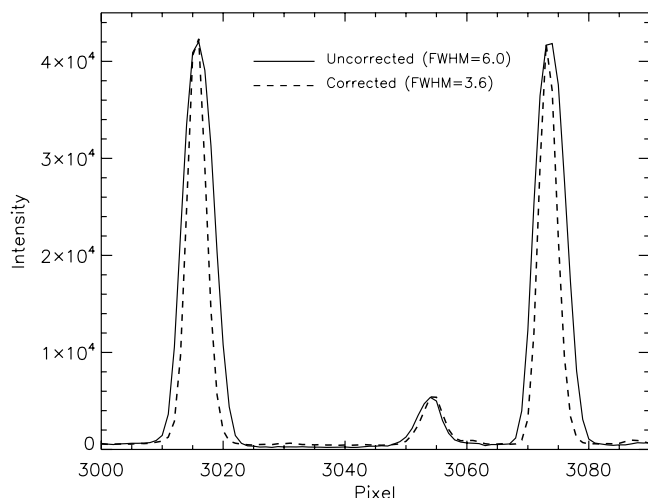
Fig. 1.—Profiles of extracted ThAr lines from the same exposure taken with Magellan-MIKE scaled to the same peak intensity. The solid line shows the ThAr lines extracted without taking into account the tilted slits. The dashed line shows the ThAr lines extracted using the mtools package. Note how the FWHM decreases when the correction is performed. [See the electronic edition of the Journal for a color version of this figure.]

A 0″.35 slit was used, providing a resolving power of 55,000 in the red and 65,000 in the blue per 4 pixel resolution element with wavelength coverage from 3800 to 8500 Å. While IRAF was used for most of the data reduction, the extraction of the Magellan data must account for the "tilted" slits; i.e., the lines are tilted with respect to the orders, and the tilt varies across the CCD. While this is a feature of all cross-dispersed echelle spectrographs, for MIKE data the tilt is severe. We used the mtools[3] set of tasks written by J. Baldwin to correct for the tilt. Failure to make this correction would result in degradation of the spectral resolution as shown in Figure 1. (The magnitude of this effect depends on the aperture size applied to the order being extracted. For the stellar spectra, the decrease in spectral resolution would be smaller than for the Th-Ar comparison spectra by roughly a factor of 2.)

3. ANALYSIS

3.1. Stellar Parameters and the Iron Abundance

The first step in the analysis was to determine the stellar parameters: the effective temperature ($T_{\rm eff}$), the surface gravity (log g), and the microturbulent velocity (ξ_t). Equivalent widths (EWs) were measured for a set of Fe I and Fe II lines using routines in IRAF. We used the same set of Fe lines presented in Y03. In Figure 2, we compare the measured EWs for Fe I and Fe II lines for the five NGC 6752 giants analyzed in Y03. The EWs measured in the Magellan data are in very good agreement with those measured in the Very Large Telescope (VLT) data. Therefore, for the five NGC 6752 giants, we adopt the same stellar parameters as used in Y03. In Figure 3, we compare the EWs of Fe I and Fe II lines for the comparison star HD 141531. The EWs measured in the Subaru data are in very good agreement with those measured in the VLT data. For HD 141531, we adopt the stellar parameters used in Y03. For the four M13 giants, we determined the stellar parameters using spectroscopic criteria. As in Y03 and Y05, the model atmospheres were taken from the Kurucz (1993) local thermodynamic equilibrium (LTE) stellar atmosphere grid and we used the LTE stellar line analysis program MOOG (Sneden 1973). For the effective temperature ($T_{\rm eff}$), we forced the Fe I lines to show no trend between abundance and lower excitation potential, i.e., excitation equilibrium. To set the surface gravity (log g), we forced the abundances from Fe I and Fe II to be equal, i.e., ionization equilibrium. We adjusted the
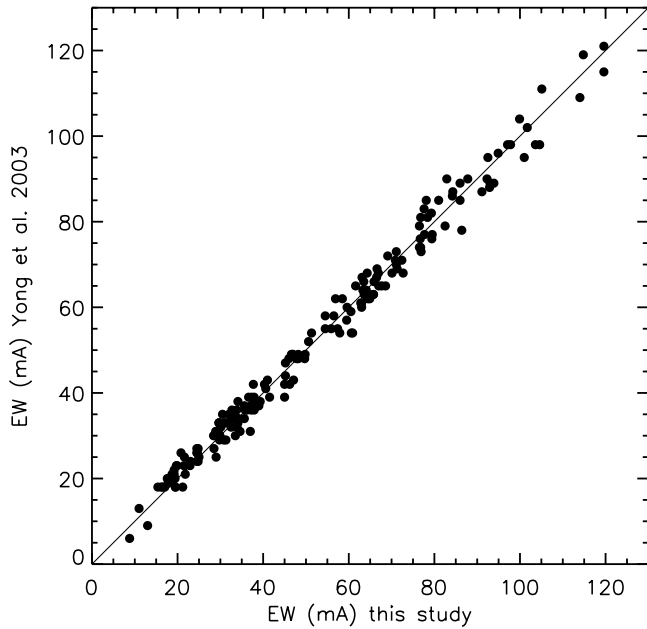
FIG. 2.—Comparison of the equivalent widths of Fe I and Fe II lines between this study (Magellan data) and Y03 (VLT data) for the sample of NGC 6752 giants.

microturbulent velocity (ξ_t) until there was no trend between abundance and EW. The final [Fe/H] was taken to be the mean of all Fe lines. Our stellar parameters for the M13 giants compare very well with those derived by Shetrone (1996a, 1996b), Sneden et al. (2004b), and Cohen & Meléndez (2005).

3.2. Rubidium Abundances

For the M13 giants, the HDS spectra did not incorporate the Rb line, so we were able to measure Rb only in the NGC 6752 giants. The abundances were determined via spectrum synthesis of the Rb I line near 7800 Å (see Figs. 4 and 5). Spectrum syn-
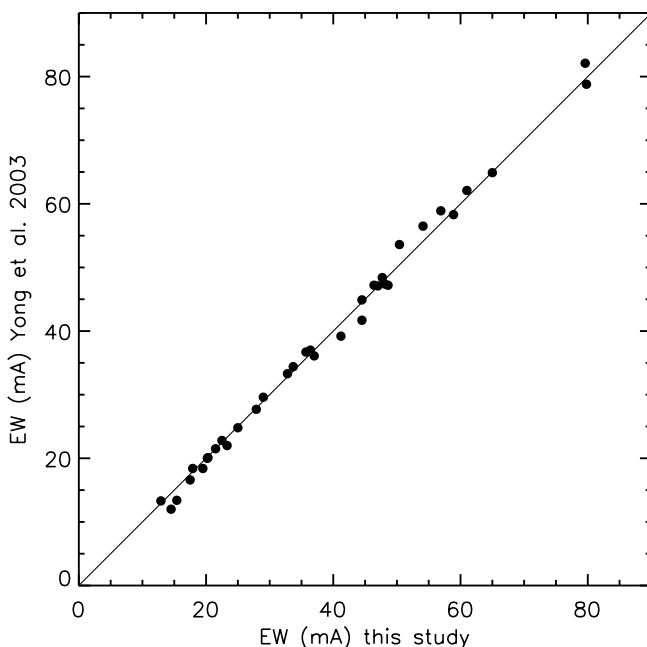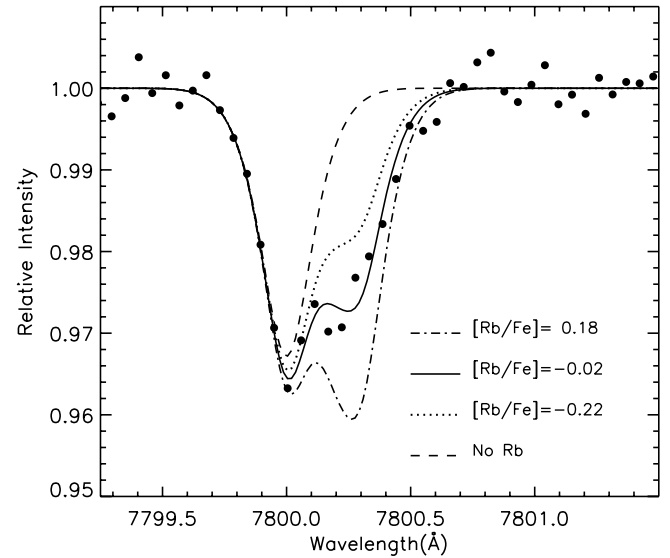

FIG. 4.—Spectrum of NGC 6752 B702 near the 7800 Å Rb feature. Synthetic spectra with differing Rb abundances are shown. [*See the electronic edition of the Journal for a color version of this figure.*]

thesis was essential for determining accurate abundances due to hyperfine splitting and isotopic shifts, as well as blending from a stronger Si I line. While the 7800 Å Rb I line is only 3%–4% deep relative to the continuum, the high-quality spectra allow us to measure an abundance from this line. Following Tomkin & Lambert (1999), the wavelengths and relative strengths for the isotopic and hyperfine-structure components were taken from Lambert & Luck (1976), and we assumed a solar isotope ratio of $^{85}Rb/^{87}Rb = 3$. The macroturbulent broadening was assumed to have a Gaussian form and was estimated by fitting the profile of the nearby Ni I line at 7798 Å. We then generated synthetic spectra and varied the Si and Rb abundances to obtain the best match to the observed spectrum. Ideally, we would like to measure the Rb isotope ratio, $^{85}Rb/^{87}Rb$, but Lambert & Luck (1976) were unable to measure accurate ratios in Arcturus even when using data with superior spectral resolution and signal-to-noise ratio (S/N) due to the presence of hyperfine structure and the
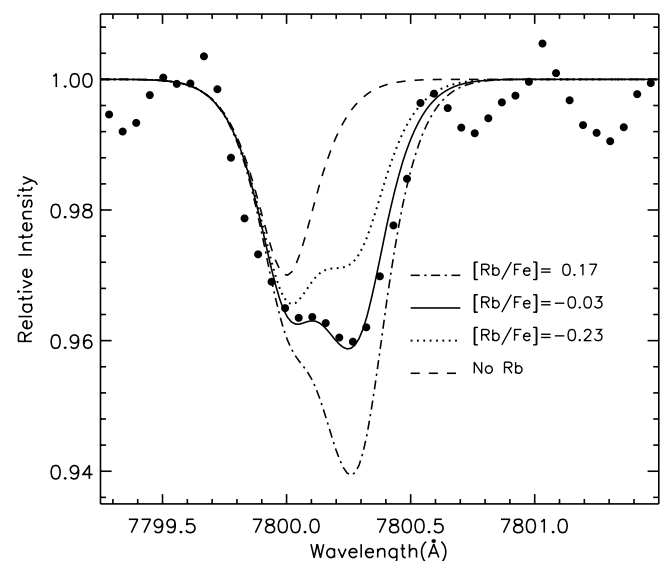

FIG. 3.—Comparison of the equivalent widths of Fe I and Fe II lines between this study (Subaru data) and Y03 (VLT data) for HD 141531.

FIG. 5.—Same as Fig. 4, but for star NGC 6752 B1630. [*See the electronic edition of the Journal for a color version of this figure.*]
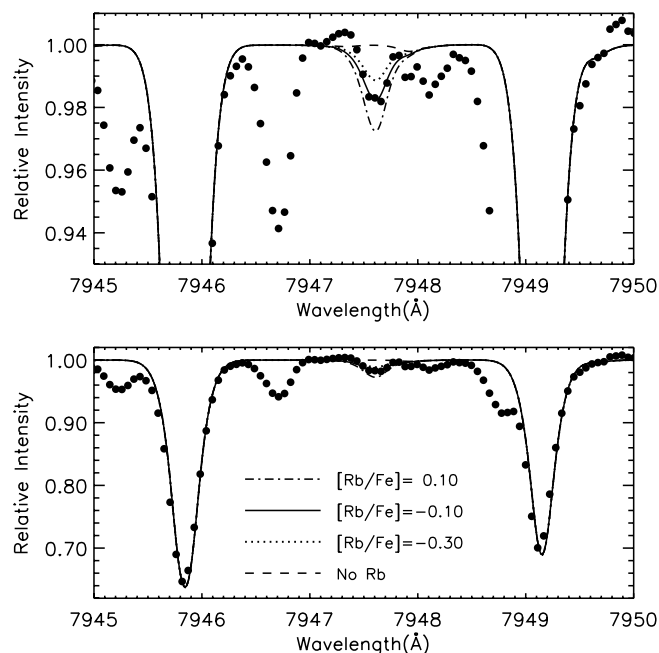
FIG. 6.—Spectrum of NGC 6752 B708 near the 7947 Å Rb feature. Synthetic spectra with differing Rb abundances are shown. The lower panel is identical to the upper panel except for the y-range. [*See the electronic edition of the Journal for a color version of this figure.*]
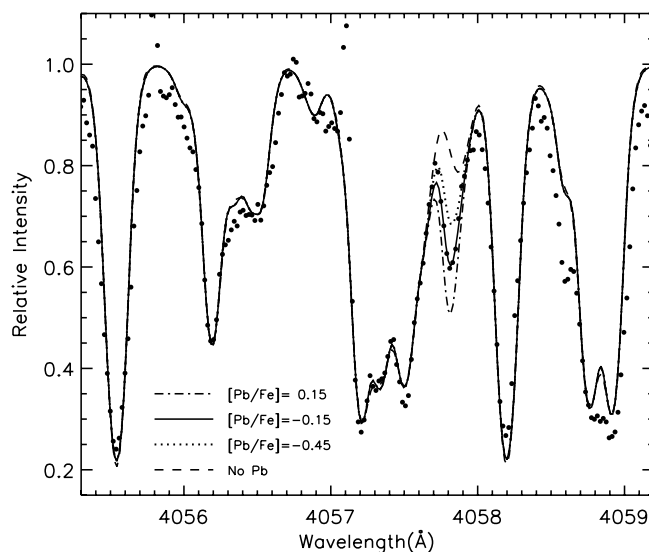

FIG. 7.—Spectrum of NGC 6752 B708 near the 4058 Å Pb feature. Synthetic spectra with differing Pb abundances are shown. [*See the electronic edition of the Journal for a color version of this figure.*]

small isotopic shift. While our tests confirmed that we could not measure accurate Rb isotope ratios, we verify the finding by Tomkin & Lambert (1999) that the derived Rb abundances are not sensitive to the assumed isotope ratio. Using the Kurucz et al. (1984) solar atlas, we measured an abundance log ϵ(Rb) = 2.58 using a model atmosphere with $T_{\rm eff}/\log g/\xi_t = 5770/4.44/0.85$. Our derived solar Rb abundance is in very good agreement with the Grevesse & Sauval (1998) value, log ϵ(Rb) = 2.60.

The subordinate Rb I line near 7947 Å is weaker by a factor of 2 and is roughly 2% deep relative to the continuum. We detect this line in all our spectra, and preliminary analyses suggest that the abundances derived from this line agree with those from the 7800 Å line (see Fig. 6). However, we prefer to restrict our results to the 7800 Å line, since the 7947 Å region is more crowded; i.e., the continuum placement strongly affects the derived Rb abundances from the 7947 Å line. Furthermore, unidentified blends, atmospheric absorption, and fringing are more prevalent in this spectral region. (CN lines that lie in this region may be absent in these metal-poor globular cluster stars.)

In the subsequent sections, we compare our globular cluster Rb abundances with field and cluster stars with [Fe/H] > −2.0 analyzed by other investigators. We now attempt to place the various Rb abundance measurements onto a common scale. While the isotope ratio of Rb cannot be measured in Arcturus, the elemental abundance ratio is well known. Using the Hinkle et al. (2000) Arcturus atlas, we measured an abundance [Rb/H] = −0.55 using a model atmosphere with $T_{\rm eff}/\log g/\xi_t = 4300/1.5/1.55$ obtained using the spectroscopic criteria described in § 3.1. The adopted Rb gf value was identical to that used by Tomkin & Lambert (1999), and our derived Rb abundance is in very good agreement with their measured value, [Rb/H] = −0.58. Since Arcturus is common to both studies and our derived abundances are essentially identical, we therefore make no adjustment to the Tomkin & Lambert Rb abundances. Gratton & Sneden (1994) use the same gf value, although the relative strengths of the hyperfine components differ slightly. We do not adjust their Rb

abundances. Abia et al. (2001) adopt a Rb gf value that differs from ours, so we adjust their Rb abundances by +0.08 dex. It is not clear what Rb gf was used by Gonzalez & Wallerstein (1998). Fortunately, Arcturus was also part of their sample. They derived an abundance [Rb/H] = −0.45, so we adjust their Rb abundances by −0.1 dex. Smith et al. (2000) find [Rb/H] = −0.52, so we do not adjust their Rb abundances.

3.3. *Lead Abundances*

The Pb abundances were determined via spectrum synthesis of the Pb I line near 4058 Å (see Figs. 7 and 8). Abundances from the Pb line near 3683 Å could not be determined due to the lack of flux in the blue for these cool giants. While the region centered near 4058 Å is crowded with molecular lines of CH, as well as atomic lines from Mg, Ti, Mn, Fe, and Co, our syntheses provide a very good fit to the region, demonstrating that reliable Pb abundances can be extracted. The macroturbulent broadening
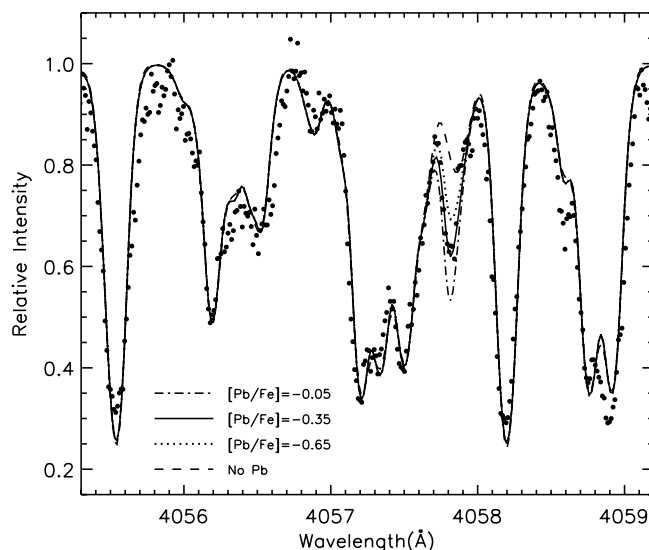

FIG. 8.—Same as Fig. 7, but for star M13 L973. [*See the electronic edition of the Journal for a color version of this figure.*]

TABLE 2
Elemental Abundances

| Star | [Al/Fe] | [Si/Fe] | [Rb/Fe] | [Y/Fe] | [Zr/Fe] | | [La/Fe] | [Eu/Fe] | [Pb/Fe] |
					Y05[a]	Smith[b]			
M13 L598	0.24	0.23	. . .	−0.10	0.27	−0.03	0.00	0.40	−0.30
M13 L629	0.74	0.31	. . .	−0.05	0.25	−0.05	0.06	0.44	−0.20
M13 L70	1.27	0.33	. . .	−0.12	0.24	−0.06	0.14	0.43	−0.27
M13 L973	1.28	0.35	. . .	−0.05	0.17	−0.13	0.12	0.52	−0.35
NGC 6752 B702....................	1.04	0.43	−0.02	0.04	0.32	0.02	0.09	0.28	−0.10
NGC 6752 B708....................	1.23	0.35	−0.22	0.04	0.30	0.00	0.03	0.28	−0.15
NGC 6752 PD1	1.08	0.38	−0.25	0.07	0.23	−0.07	0.07	0.32	−0.30
NGC 6752 B1630..................	0.82	0.41	−0.03	0.04	0.19	−0.11	0.05	0.34	−0.10
NGC 6752 B3589..................	0.77	0.43	−0.32	0.10	0.20	−0.10	0.08	0.35	−0.18
HD 141531	0.01	0.23	. . .	−0.13	0.14	−0.16	0.00	0.33	−0.20

[a] Zr abundances using the *gf* values and solar abundance assumed in Y05.
[b] Zr abundances when shifted onto the Smith et al. (2000) scale.

was estimated by fitting the profiles of the nearby lines. We adopted the same *gf* value as used by Aoki et al. (2000, 2001, 2002). Following Aoki et al. (2002), our synthesis accounted for the hyperfine and isotopic splitting, as well as the isotopic shifts. (The stable isotopes are ^{204}Pb, ^{206}Pb, ^{207}Pb, and ^{208}Pb.) We again assumed a solar isotope ratio for Pb, although as with Rb, our tests confirmed that the derived elemental Pb abundance was not sensitive to this choice. For the solar Pb abundance, we adopted $\log \epsilon(\mathrm{Pb}) = 1.95$ from Grevesse & Sauval (1998).

In the subsequent sections, we compare the globular cluster Pb abundances with those obtained in field stars with [Fe/H] > −2.0 by other investigators. However, we further restrict the comparison by avoiding stars with known *s*-process enhancements, leaving only a handful of stars from two studies, Sneden et al. (1998) and Travaglio et al. (2001). Again we attempt to put the Pb abundance measurements onto a common scale. Our *gf* value is identical to that used by Sneden et al. (1998), so we do not adjust their Pb abundances. Travaglio et al. (2001) used a different Pb line (3683 Å) and did not list the adopted *gf* value. Since there are no stars common to both analyses, we do not make an adjustment to their Pb abundances and caution that there may be a systematic offset.

3.4. *Additional Elements*

We also measured abundances for Al, Si, Y, Zr, La, and Eu in the M13 giants and the comparison star HD 141531 using the same lines as presented in Y05. These measurements were performed to ensure that the abundances would be on the same scale as the NGC 6752 giants studied in Y05. Zr was chosen because we compare the Rb and Zr abundances to look for a large ratio [Rb/Zr], as well as a detectable dispersion, i.e., the hallmark of a high neutron density environment and the possible signature of pollution from IM-AGBs. Al, Si, and Y were also chosen because Y05 found evidence for correlations between Al and Si, Al and Y, and Al and Zr in NGC 6752. While our sample size in M13 is small, it would be interesting to see whether similar correlations are present. La and Eu were measured, since these neutron-capture elements offer an insight into the ratio of *s*-process to *r*-process material. Furthermore, the ratio [Pb/La] has been used to test predictions from AGB models. In Table 2 we present our measured elemental abundances for Al, Si, Rb, Y, Zr, La, Eu, and Pb in the program stars. The adopted solar abundances for Al, Si, Y, Zr, La, and Eu were 6.47, 7.55, 2.24, 2.60, 1.13, and 0.52, respectively.

We attempt once more to put the abundance measurements onto a common scale by considering the *gf* values used by the various studies to which we compare our abundances. The element that we focus on is Zr (in order to compare [Rb/Zr] between the samples). We shift all the Zr abundances onto the Smith et al. (2000) scale in order to compare with their theoretical predictions for [Rb/Zr] from low- and intermediate-mass AGBs (their Fig. 14). (Our Rb abundances were already on the Smith scale.) Abundance measurements for Zr are complicated by the fact that the laboratory Zr *gf* values from Biémont et al. (1981) are smaller than the solar *gf* values by 0.41 dex (Tomkin & Lambert 1999). We must therefore take care and account for both the adopted solar abundance and the *gf* value. Smith et al. (2000) adopt the Biémont et al. (1981) *gf* values and a solar abundance $\log \epsilon_{\odot}(\mathrm{Zr}) = 2.90$. We used the Biémont et al. (1981) *gf* values and a solar abundance $\log \epsilon_{\odot}(\mathrm{Zr}) = 2.60$ (Grevesse & Sauval 1998). Therefore, we adjust our Zr abundances by −0.30 dex to ensure that we are on the same scale as Smith et al. (2000). Similarly, we adjust the Zr abundances of Gratton & Sneden (1994) and Abia et al. (2001) by −0.30 dex, since they adopt the same *gf* values and a solar abundance very similar to that used in our analysis. Gonzalez & Wallerstein (1998) adopt the Grevesse & Sauval (1998) solar abundance and a different *gf* value, so we adjust their Zr abundances by +0.06 dex. Tomkin & Lambert (1999) adopt the Grevesse & Sauval (1998) solar abundance and a different *gf* value, so we adjust their Zr abundances by +0.11 dex. These adjustments are substantial. When we compare the ratio [Rb/Zr], we also consider how the comparison would fare had we not made these abundance corrections. To assess the validity of these adjustments, we measured the Zr abundance for Arcturus and found [Zr/H] = −0.66. Smith et al. measured [Zr/H] = −0.96, Gonzalez & Wallerstein found −1.18, and Tomkin & Lambert found −1.00. Therefore, applying the abundance corrections based on the *gf* values and solar abundances ensures that the Zr abundances are on the Smith et al. (2000) scale, e.g., for Arcturus we find −0.96 (this study), −1.12 (Gonzalez & Wallerstein), −0.89 (Tomkin & Lambert), and −0.96 (Smith et al.). Interestingly, if we had used the same solar abundance as Smith et al. (2000), our [Zr/Fe] abundances in Y05 would have been closer to the [Y/Fe] values and for M13 we would have found [Y/Fe] ≃ [Zr/Fe]. In Figure 9, we plot [Zr/Fe] versus [Fe/H] with the abundances shifted to the Smith et al. (2000) scale. At the metallicity of NGC 6752 and M13, the field and cluster stars have similar ratios of [Zr/Fe]. The comparison
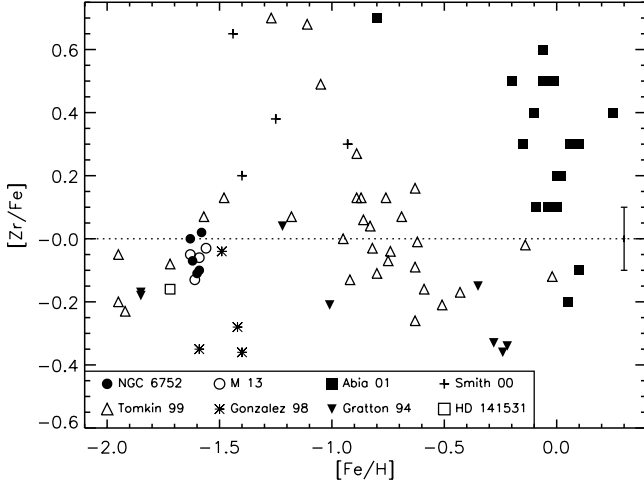
FIG. 9.—[Zr/Fe] vs. [Fe/H]. Filled circles show our measurements for NGC 6752, the open circles show M13, the open square shows HD 141531, the filled triangles are from Gratton & Sneden (1994), the asterisks represent data from Gonzalez & Wallerstein (1998), open triangles are from Tomkin & Lambert (1999), plus signs represent data from Smith et al. (2000), and filled squares show data from Abia et al. (2001). A representative error bar is shown, and the Zr abundances have been shifted onto the Smith et al. scale (see text for details). [*See the electronic edition of the Journal for a color version of this figure.*]
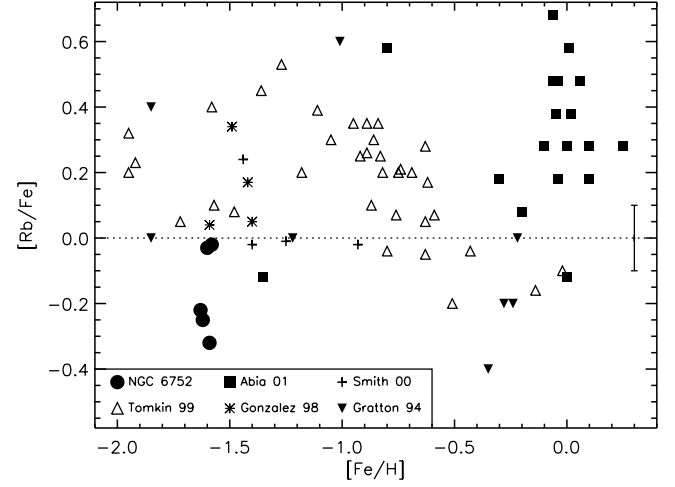

FIG. 10.—[Rb/Fe] vs. [Fe/H]. Filled circles show our measurements for NGC 6752, the filled triangles are from Gratton & Sneden (1994), the asterisks represent data from Gonzalez & Wallerstein (1998), open triangles are from Tomkin & Lambert (1999), plus signs represent data from Smith et al. (2000), and filled squares show data from Abia et al. (2001). A representative error bar is shown. [*See the electronic edition of the Journal for a color version of this figure.*]

field star HD 141531 has [Zr/Fe] almost identical to that of the globular clusters.

As in Y03, we estimate the internal errors in the stellar parameters to be $T_{\rm eff} \pm 50$ K, $\log g \pm 0.2$, and $\xi_t \pm 0.2$. In Table 3, we show the abundance dependences on the model parameters.

4. DISCUSSION

4.1. *Rubidium*

While our mean Rb abundance for NGC 6752 is [Rb/Fe] = -0.17 ± 0.06 ($\sigma = 0.14$), the abundances appear to concentrate around two distinct values. There are two stars with [Rb/Fe] $\simeq$ -0.02 and three stars with [Rb/Fe] $\simeq -0.25$. The two stars with the higher Rb abundances do not have the highest Al abundances, and the three stars with the lower Rb abundances are not exclusively the stars with the lowest Al abundances. Given the weakness of the Rb line, the uncertainties in the derived Rb abundances (see Table 3), and the small sample size, it is unlikely that the Rb abundances show a dispersion in NGC 6752. Nor do we find evidence for a correlation between [Al/Fe] and [Rb/Fe], although we recognize that our sample size (5 stars) is much more limited than that in Y03 and Y05 (38 stars). Unfortunately,

observations of M13 and the comparison field star HD 141531 did not incorporate the Rb line.

In Figure 10, we compare our Rb abundances with those measured in dwarfs and giants in the disk and halo (Gratton & Sneden 1994; Tomkin & Lambert 1999), globular cluster giants (Gonzalez & Wallerstein 1998; Smith et al. 2000), and carbon-rich AGB stars (Abia et al. 2001). (While we retain their stars in the plots, we note that the Abia sample contains very different objects that are difficult to analyze compared to the dwarfs and giants considered in the other studies.) Recall that we have made small adjustments to the Rb abundances in an attempt to place them onto a common scale. At the metallicity of NGC 6752 ([Fe/H] = -1.6), our two stars in NGC 6752 with the highest [Rb/Fe] ratios have abundances compatible with the lower envelope of the Tomkin & Lambert (1999) sample. The two NGC 6752 stars also exhibit abundance ratios [Rb/Fe] very similar to those of the Gonzalez & Wallerstein (1998) and Smith et al. (2000) globular cluster giants. Our three stars with the lower [Rb/Fe] ratios seem unusual compared to the Tomkin & Lambert sample. Only one star in the Abia et al. (2001) sample has [Fe/H] < -1.0, and it is interesting that it has an abundance ratio [Rb/Fe] similar to those measured in NGC 6752. In general, Rb is not a well-studied element, and the comparison data are limited.

For NGC 6752, we find a mean abundance [Rb/Zr] = -0.12 ± 0.06 ($\sigma = 0.13$). (This abundance ratio has been shifted to the Smith et al. [2000] scale.) For the five NGC 6752 giants, the ratio [Rb/Zr] appears to show a dispersion. We suspect that this is attributable to measurement uncertainties (primarily for Rb) rather than reflecting a real star-to-star scatter. We do not find a correlation between [Al/Fe] and [Rb/Zr]. In Figure 11, we compare the abundance ratio [Rb/Zr] between NGC 6752 and various field and cluster stars. Note that in this figure we have shifted all abundances onto the Smith et al. (2000) scale, since we utilize their theoretical predictions from low- and intermediate-mass AGBs. At the metallicity of NGC 6752, we find that the two stars in NGC 6752 with the highest values of [Rb/Fe] also have the highest values of [Rb/Zr]. These two stars have [Rb/Zr] ratios similar to those of the Gratton & Sneden (1994) and Tomkin &

TABLE 3
ABUNDANCE DEPENDENCES ON MODEL PARAMETERS FOR NGC 6752 B1630

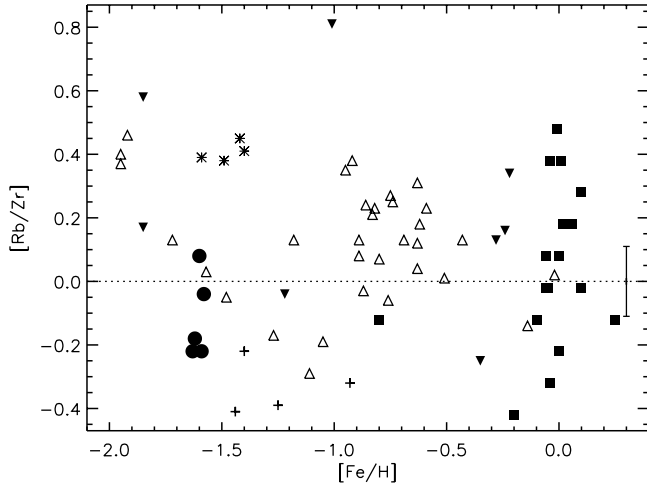| Species	$T_{\rm eff} + 50$ (K)	$\log g + 0.2$ (cgs)	$\xi_t + 0.2$ (km s^{-1})
[Fe/H]	0.02	0.01	-0.03
[Al/Fe]	0.05	-0.01	-0.01
[Si/Fe]	-0.01	0.03	-0.01
[Rb/Fe]	0.09	0.03	-0.01
[Y/Fe]	0.01	0.06	-0.04
[Zr/Fe]	0.13	0.02	-0.01
[La/Fe]	-0.02	0.05	-0.05
[Eu/Fe]	-0.04	0.05	-0.04
[Pb/Fe]	0.12	-0.05	-0.02

FIG. 11.—[Rb/Zr] vs. [Fe/H]. The symbols are the same as in Fig. 10. Note that we shifted all abundances onto the Smith et al. (2000) scale (see text for details). [*See the electronic edition of the Journal for a color version of this figure.*]

Lambert (1999) samples at the same metallicity. While the ω Cen giants have abundance ratios [Rb/Zr] slightly lower than NGC 6752, this time the NGC 3201 giants appear to have much higher ratios of [Rb/Zr]. Note that the [Rb/Zr] ratios in NGC 3201 appear similar to the highest values seen in the Tomkin & Lambert (1999) sample. Unfortunately, the only star in the Abia et al. (2001) sample with [Fe/H] < -1.0 does not have a Zr measurement. However, it does have [Rb/Sr] $= -0.5$ and [Rb/Y] $= -0.6$. If we assume for this star [Rb/Zr] $= \langle$[Rb/Sr], [Rb/Y]$\rangle = -0.55$, then the abundance is much lower than that of NGC 6752.

For elements heavier than Si, globular clusters and field stars tend to have very similar abundance ratios [X/Fe] at a given [Fe/H] (Gratton et al. 2004; Sneden et al. 2004a). Although the scatter is large and the sample sizes are limited, it would appear that cluster stars probably have similar or perhaps slightly lower abundance ratios of [Rb/Fe] and [Rb/Zr] compared to field stars at a given [Fe/H].

Recall that we made substantial adjustments to the Zr abundance. While consideration of the Arcturus Zr abundances would appear to validate this adjustment, we briefly consider how the comparison of [Rb/Zr] would have fared if these corrections had not been applied. In this case, the ratio [Rb/Zr] would decrease by roughly 0.3 dex for NGC 6752, as well as for the Gratton & Sneden (1994) and Abia et al. (2001) samples. The Tomkin & Lambert (1999) and Gonzalez & Wallerstein (1998) samples would increase by roughly 0.15 dex. NGC 6752 would therefore have unusually low ratios [Rb/Zr] compared to field stars at the same metallicity. Similarly, the ω Cen compositions would be unusually low although comparable to NGC 6752. The NGC 3201 giants would then have very high [Rb/Zr] ratios compared to other globular clusters and field stars at the same metallicity. NGC 3201 is peculiar, since it has a retrograde orbit and may have been a captured cluster (van den Bergh 1993). The capture hypothesis could not be demonstrated by Gonzalez & Wallerstein (1998), who found no unusual abundance ratios.

Smith et al. (2000) compare [Rb/Zr] in ω Cen with predictions from AGB models with various initial masses and initial metallicities (their Fig. 14). Their figure clearly shows how the ratio [Rb/Zr] can vary by nearly a factor of 10 depending on whether a low-mass (1.5 $M_\odot$) or high-mass (5 $M_\odot$) AGB model is synthesizing the s-process elements. As anticipated from the arguments given in § 1, high-mass AGB models produce high [Rb/Zr]

while low-mass AGB models produce low [Rb/Zr]. The magnitude of the difference in the predicted [Rb/Zr] between low- and high-mass AGB models does not significantly change as the metallicity decreases from [Fe/H] $= -0.5$ to -2.0. Comparing the observed abundances with the model predictions in Smith et al. reveals that low-mass AGB stars (1–3 $M_\odot$) are responsible for the synthesis of the s-process elements in ω Cen. Inspection of Figure 14 in Smith et al. (2000) shows that at the metallicity of NGC 6752, [Fe/H] $= -1.6$, our measured ratio [Rb/Zr] $= -0.12$ is compatible with the s-process elements being synthesized in low-mass AGB stars, although the assumed mass of the ^{13}C pocket is critical. Predictions assuming a standard treatment for the ^{13}C pocket or the ^{13}C pocket increased by a factor of 2 both suggest that AGB stars with <3 $M_\odot$ are responsible for the [Rb/Zr] ratios seen in NGC 6752. When the ^{13}C pocket is diminished by a factor of 3, the AGB stars with masses >3 $M_\odot$ may explain the observed [Rb/Zr]. When we return our Zr abundances to the original scale, [Rb/Zr] $= -0.42$, the ratio in NGC 6752 is only compatible with low-mass AGB stars. We note that the highest values of [Rb/Zr] seen in the Gratton & Sneden (1994), Gonzalez & Wallerstein (1998), and Tomkin & Lambert (1999) samples all greatly exceed the 5 $M_\odot$ AGB model predictions. Such a discrepancy serves as a useful reminder of the unfortunate reality that the detailed yields of s-process elements from AGB stars may be very model dependent (Busso et al. 2001; Ventura & D'Antona 2005).

4.2. Lead

In NGC 6752 the mean Pb abundance is [Pb/Fe] $= -0.17 \pm 0.04$ ($\sigma = 0.08$), and in M13 the mean abundance is [Pb/Fe] $= -0.28 \pm 0.03$ ($\sigma = 0.06$). Given the fairly large measurement uncertainty for Pb (see Table 3), neither NGC 6752 nor M13 shows any evidence for a dispersion in Pb abundances, although our sample sizes for both clusters are small. Furthermore, the [Pb/Fe] ratios are very similar for these two clusters. As with Rb, there is no evidence that the ratio [Pb/Fe] is correlated with [Al/Fe]. We note that one star, NGC 6752 PD1, has lower ratios of both [Rb/Fe] and [Pb/Fe] relative to other giants in this cluster. This subtle composition difference probably arises from uncertainties in the stellar parameters rather than representing a genuine difference. The comparison field giant HD 141531 has a ratio [Pb/Fe] essentially identical to those of the globular cluster giants.

In Figure 12, we compare our Pb abundances with values measured by Sneden et al. (1998) and Travaglio et al. (2001). While Pb has been measured in numerous stars with large s-process enhancements, it has been largely neglected in normal field stars, presumably due to the difficulty of the measurement. For HD 126238, the Pb abundance measured by Sneden et al. (1998) is very similar to those of the globular cluster giants and HD 141531. The Pb abundances measured by Travaglio et al. (2001) in field stars are larger than those measured in the globular clusters. The star with [Pb/Fe] $= 0.6$ is a CH star with excess C and Ba and should not be considered a normal field star. Aside from the CH star, there are three stars with upper limits and another three Pb detections. Recall that there are no stars common to both studies and that the Pb gf value was not published. Travaglio et al. (2001) suggest that some of the Pb detections may be uncertain and, therefore, the offset between the Pb abundances may be due to measurement errors and/or the adopted gf value.

Travaglio et al. (2001) not only measured Pb abundances in a handful of stars, but they calculated the Galactic chemical evolution of Pb from a detailed model. In their Figure 4, they plot the expected run of [Pb/Fe] versus [Fe/H] for the halo, thick disk,
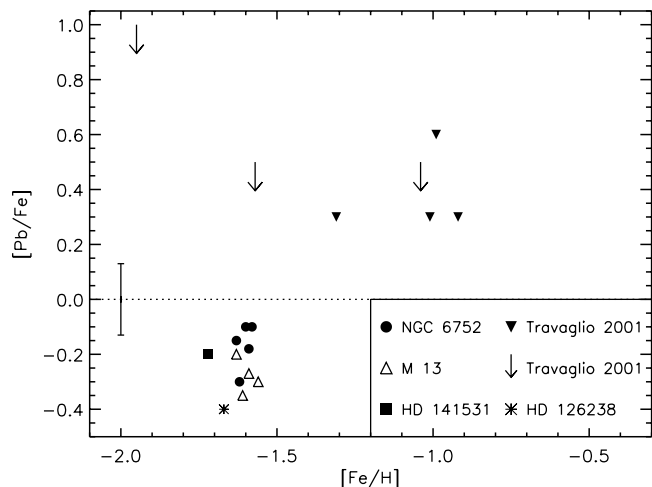
Fig. 12.—[Pb/Fe] vs. [Fe/H]. Filled circles, open triangles, and the filled square show our measurements for NGC 6752, M13, and the comparison field star HD 141531. The filled triangles and arrows (upper limits) are from Travaglio et al. (2001), while the asterisk shows HD 126238 from Sneden et al. (1998). A representative error bar is shown. [*See the electronic edition of the Journal for a color version of this figure.*]

and thin disk. Since their prediction integrates over all Stellar masses, it would be useful to learn how the predicted curve would differ (if at all) if the calculation was performed using low-mass or high-mass AGB models exclusively as Smith et al. (2000) have done. At $[Fe/H] = -1.6$, the Travaglio et al. (2001) model predicts an abundance ratio $[Pb/Fe] \simeq -0.1$. This prediction is in very good agreement with the values measured in M13, NGC 6752, HD 126238, and HD 141531. This agreement can be regarded as evidence that globular cluster stars have Pb abundances virtually identical to those of normal field stars.

In normal field stars, Pb has been less studied than Rb. Clearly, it would be of great interest to have additional Pb measurements in field and cluster stars. In Figures 7 and 8, our syntheses indicate that for cool giants in the metallicity regime $-2.0 < [Fe/H] < -1.0$, reliable Pb abundances can be measured even in stars that do not have large Pb or s-process enhancements.

The ratio $[Pb/La]$ may offer further clues regarding the nature of the s-process in the AGB stars. Van Eck et al. (2003) found some stars with ratios of $[Pb/La] > +1.5$, in agreement with predictions from metal-poor AGB models (Gallino et al. 1998; Goriely & Mowlavi 2000). However, Aoki et al. (2002) and Van Eck et al. (2003) also found a large spread in the ratio $[Pb/Ba]$. In some stars, the ratio $[Pb/Ba]$ was subsolar. Our mean ratio $[Pb/La]$ for M13 is -0.36 ± 0.05 ($\sigma = 0.10$). For NGC 6752, our mean ratio $[Pb/La] = -0.23 \pm 0.04$ ($\sigma = 0.09$). In both clusters, the mean ratios are similar, and we note that they are both subsolar and comparable to the lowest ratios seen in the Van Eck et al. (2003) sample. Curiously, the subsample in Van Eck et al. (2003) with $[Pb/La] < 0$ had extreme enhancements for $[Pb/Fe]$ and $[La/Fe]$. The comparison field star HD 141531 has $[Pb/La] = -0.20$, which is similar to the value seen in the globular clusters.

4.3. Additional Elements

While our sample in M13 consists of only four stars, they span the extremities of the Al variation. As in Y05, we again find that the most Al-rich stars may also exhibit slightly higher Si abundances than the most Al-poor stars. Further measurements of Al and Si in a large sample of stars in M13 would be of great interest to verify whether the correlation between Al and Si seen in NGC 6752 (Y05) is also present in M13. The correlations between Al

and Y, as well as Al and Zr, found in NGC 6752 do not appear to be present in the small M13 sample. Cohen & Meléndez (2005) measured abundances in 25 stars in M13 from the main-sequence turnoff to the tip of the RGB. They were unable to measure Al in most stars. When we consider their derived abundances, there appears to be an anticorrelation between O and Si, as well as O and Y. Although the anticorrelation is driven primarily by the one star with unusually low [O/Fe], such trends are intriguing and warrant further investigation.

As noted in previous investigations of these clusters, the ratio of s-process to r-process material, [La/Eu], is subsolar but greater than the scaled solar pure r-process value. For NGC 6752 and M13, the observed ratios of [La/Eu] show that AGB stars have contributed to their chemical evolution. The ratio of La/Eu in HD 141531 again confirms that it is a normal field star.

4.4. Consequences for the IM-AGB Pollution Scenario

In Y03, we measured Mg isotope ratios in bright giants in NGC 6752. We found that the ratio varied from star to star. Specifically, ^{24}Mg was anticorrelated with Al, ^{26}Mg was correlated with Al, and ^{25}Mg was not correlated with Al. As previously seen by Shetrone (1996b) in M13, these isotope ratios reveal that the Al enhancements result from proton capture on the abundant ^{24}Mg. Proton capture on ^{24}Mg within the Mg-Al chain is predicted to occur only in AGB stars of the highest mass at their maximum luminosity (Karakas & Lattanzio 2003). Thus, we suggested that the abundance variations were due to differing degrees of pollution by IM-AGBs, an idea originally proposed by Cottrell & Da Costa (1981). These IM-AGBs must have the same iron abundance as the present generation of cluster stars; otherwise, there would also be a star-to-star abundance variation of Fe. (The same argument applies to whatever stars are believed to be the source of the pollutants.)

The Mg isotope ratios presented in Y03 offered further clues to globular cluster chemical evolution. At one extreme of the abundance variation are cluster stars with O, Na, Mg, and Al compositions in accord with field stars at the same metallicity. We called such stars "normal" in anticipation that proton-capture nucleosynthesis can produce O-poor, Na-rich, Mg-poor, and Al-rich material. At the other extreme of the abundance variations are the stars with high Na, high Al, low O, and low Mg. We referred to these stars as "polluted." The pollution may have occurred via either the evolutionary or primordial scenario. In "normal" stars, we found ratios ^{25}Mg/^{24}Mg and ^{26}Mg/^{24}Mg that exceeded those of field stars at the same metallicity (Yong et al. 2003b). Of equal importance was the fact that these isotope ratios greatly exceeded predictions from metal-poor supernovae. We therefore suggested that these unusually high isotope ratios could be explained if a previous generation of IM-AGBs of the highest mass polluted the natal cloud from which the cluster formed. The ejecta from this previous generation must have been thoroughly mixed before the present generation of stars began to form. This previous generation of IM-AGBs is probably responsible for much of the Na, Al, and N, as well as ^{25}Mg and ^{26}Mg.

Our working hypothesis is that IM-AGBs played two crucial roles in globular cluster chemical evolution. First, a prior generation of very metal-poor IM-AGBs are required to produce the high ^{25}Mg/^{24}Mg and ^{26}Mg/^{24}Mg seen in "normal" stars. Second, a generation of IM-AGBs with the same Fe abundance as the present cluster members pollutes the cluster environment. Differing degrees of pollution of natal clouds then produce the star-to-star abundance variations. The dispersion in the F abundances and the correlation between F and O in M4 (Smith et al. 2005) appear to confirm the role of IM-AGBs in producing the

abundance variations. However, not all the abundance patterns observed in globular clusters can be matched by the current theoretical yields from IM-AGBs (Denissenkov & Herwig 2003; Denissenkov & Weiss 2004), nor can the abundance patterns be reproduced by chemical evolution models (Fenner et al. 2004).

From a qualitative viewpoint, metal-poor IM-AGBs may produce s-process elements via the ^{22}Ne neutron source. If activated, the ^{22}Ne neutron source produces large amounts of Rb/Zr due to a critical branching point at ^{85}Kr as described earlier. Theoretical models by Busso et al. (2001) suggest that metal-poor IM-AGBs do run the s-process, although the specific yields depend on the details.

Similarly, a qualitative assessment suggests that metal-poor IM-AGBs will produce Bi and Pb if the neutrons per seed nucleus exceed a certain value. In this case, Bi and Pb may show large enhancements with other s-process elements showing only modest overabundances. Again, theoretical models can be found in which metal-poor IM-AGBs do produce lead (e.g., Goriely & Siess 2001; Busso et al. 2001).

In M13 and NGC 6752, we did not find high ratios of $[\mathrm{Rb/Fe}]$, $[\mathrm{Rb/Zr}]$, or $[\mathrm{Pb/Fe}]$ compared with field stars at the same metallicity. If metal-poor IM-AGBs are responsible for the globular cluster star-to-star abundance variations, then our measurements strongly suggest that such stars do not synthesize significant quantities of Rb or Pb. Also, if metal-poor IM-AGBs are responsible for the large abundances of ^{25}Mg and ^{26}Mg in "normal" cluster stars, then they do not synthesize Rb or Pb. Alternatively, if metal-poor IM-AGBs do synthesize significant quantities of Rb and Pb, then they cannot be responsible for the abundance anomalies seen in globular clusters.

Of course, the possibility remains that the predicted yields of Rb and Pb from IM-AGBs are unreliable and/or model dependent (e.g., Ventura & D'Antona 2005). It has been suggested that metal-poor IM-AGBs will not produce any s-process elements. As the mass of the AGB star increases, the size of the He intershell region decreases as does the duration of the thermal pulse (Lattanzio et al. 2004). Detailed predictions of the yields from metal-poor IM-AGBs by independent groups are required. Our observed Rb and Pb abundances may serve to constrain these models.

Finally, we note that Rb and Zr are synthesized in IM-AGBs, as well as via the weak s-process, i.e., He core burning in massive stars. However, Travaglio et al. (2004) suggest that the weak s-process does not contribute to Zr but a lighter element primary process in massive stars may be responsible for up to 18% of the solar abundance of Zr. Chieffi & Limongi (2004) present detailed yields from massive stars for a range of metallicities and masses. At $Z = 0$, massive stars are predicted to produce low ratios, $[\mathrm{Rb/Zr}] = -0.5$ to -2.4. If IM-AGBs have contributed to the chemical evolution of NGC 6752, they would increase the ratios of [Rb/Zr] above those produced by the supernovae. If IM-AGBs have not played a role in the chemical evolution, perhaps we can use [Rb/Zr] to probe the mass and metallicity

range of the previous generation of massive stars. For $Z = 10^{-4}$, the predicted yields are independent of mass with $[\mathrm{Rb/Zr}] = -0.23$. However, we note that for other metallicities, there is a mass-metallicity degeneracy for the [Rb/Zr] yields that limits their use in probing the previous generation of supernovae.

5. CONCLUDING REMARKS

We show for the first time the uniformity of the neutron-capture elements Rb and Pb in NGC 6752 and M13, the two globular clusters that exhibit the largest dispersion for Al. We also find the ratio $[\mathrm{Rb/Zr}]$ to be constant. None of the abundance ratios $[\mathrm{Rb/Fe}]$, $[\mathrm{Rb/Zr}]$, or $[\mathrm{Pb/Fe}]$ are correlated with $[\mathrm{Al/Fe}]$, and the Rb and Pb abundances show subsolar ratios $[\mathrm{X/Fe}]$. If metal-poor IM-AGBs produce large amounts of Pb and Rb, as well as high ratios of $[\mathrm{Rb/Zr}]$, then such stars are not responsible for the abundance variations, a conclusion already suggested by Denissenkov & Herwig (2003), Denissenkov & Weiss (2004), and Fenner et al. (2004). If metal-poor IM-AGBs are responsible for the abundance variations, then they cannot produce overabundances of Rb or Pb.

For elements heavier than Al, previous studies have shown that field and cluster stars generally have the same abundance ratios $[\mathrm{X/Fe}]$ at a given $[\mathrm{Fe/H}]$. While our sample size is small and the data for comparison field stars are limited, the two clusters we have studied have Rb abundance ratios $[\mathrm{Rb/Fe}]$ and $[\mathrm{Rb/Zr}]$ in reasonable agreement with the general field population (the clusters may have slightly lower ratios). The Pb abundance ratio $[\mathrm{Pb/Fe}]$ in globular clusters is in very good agreement with the limited sample of field stars. At the metallicity of M13 and NGC 6752, their Pb abundances are well matched by the predictions from the chemical evolution model by Travaglio et al. (2001). In order to further our understanding of stellar nucleosynthesis and the chemical evolution of field and cluster stars, additional measurements of Rb and Pb in normal stars and globular clusters are welcomed, as are further theoretical efforts to calculate the yields from metal-poor IM-AGBs.

REFERENCES

Abia, C., Busso, M., Gallino, R., Domínguez, I., Straniero, O., & Isern, J. 2001, ApJ, 559, 1117
Aikawa, M., Fujimoto, M. Y., & Kato, K. 2001, ApJ, 560, 937
———. 2004, ApJ, 608, 983
Aoki, W., Norris, J. E., Ryan, S. G., Beers, T. C., & Ando, H. 2000, ApJ, 536, L97
Aoki, W., Ryan, S. G., Norris, J. E., Beers, T. C., Ando, H., & Tsangarides, S. 2002, ApJ, 580, 1149
Aoki, W., et al. 2001, ApJ, 561, 346
Beer, H., & Macklin, R. L. 1989, ApJ, 339, 962

Bernstein, R., Shectman, S. A., Gunnels, S. M., Mochnacki, S., & Athey, A. E. 2003, Proc. SPIE, 4841, 1694
Biémont, E., Grevesse, N., Hannaford, P., & Lowe, R. M. 1981, ApJ, 248, 867
Burris, D. L., Pilachowski, C. A., Armandroff, T. E., Sneden, C., Cowan, J. J., & Roe, H. 2000, ApJ, 544, 302
Busso, M., Gallino, R., Lambert, D. L., Travaglio, C., & Smith, V. V. 2001, ApJ, 557, 802
Busso, M., Gallino, R., & Wasserburg, G. J. 1999, ARA&A, 37, 239
Charbonnel, C. 1995, ApJ, 453, L41
Chieffi, A., & Limongi, M. 2004, ApJ, 608, 405

Cohen, J. G. 1978, ApJ, 223, 487

Cohen, J. G., & Meléndez, J. 2005, AJ, 129, 303

Cottrell, P. L., & Da Costa, G. S. 1981, ApJ, 245, L79

Cowan, J. J., Sneden, C., Truran, J. W., & Burris, D. L. 1996, ApJ, 460, L115

Denissenkov, P. A., & Herwig, F. 2003, ApJ, 590, L99

Denissenkov, P. A., & Weiss, A. 2004, ApJ, 603, 119

Fenner, Y., Campbell, S., Karakas, A. I., Lattanzio, J. C., & Gibson, B. K. 2004, MNRAS, 353, 789

Fujimoto, M. Y., Aikawa, M., & Kato, K. 1999, ApJ, 519, 733

Gallino, R., Arlandini, C., Busso, M., Lugaro, M., Travaglio, C., Straniero, O., Chieffi, A., & Limongi, M. 1998, ApJ, 497, 388

Gonzalez, G., & Wallerstein, G. 1998, AJ, 116, 765

Goriely, S., & Mowlavi, N. 2000, A&A, 362, 599

Goriely, S., & Siess, L. 2001, A&A, 378, L25

Gratton, R., Sneden, C., & Carretta, E. 2004, ARA&A, 42, 385

Gratton, R. G., & Sneden, C. 1994, A&A, 287, 927

Gratton, R. G., et al. 2001, A&A, 369, 87

Grevesse, N., & Sauval, A. J. 1998, Space Sci. Rev., 85, 161

Grundahl, F., Briley, M., Nissen, P. E., & Feltzing, S. 2002, A&A, 385, L14

Herwig, F. 2004, ApJ, 605, 425

Hinkle, K., Wallace, L., Valenti, J., & Harmer, D. 2000, Visible and Near Infrared Atlas of the Arcturus Spectrum 3727–9300 Å (San Francisco: ASP)

Ivans, I. I., Sneden, C., Gallino, R., Cowan, J. J., & Preston, G. W. 2005, ApJ, 627, L145

Johnson, J. A., & Bolte, M. 2002, ApJ, 579, L87

Karakas, A. I., & Lattanzio, J. C. 2003, Publ. Astron. Soc. Australia, 20, 279

Kraft, R. P. 1994, PASP, 106, 553

Kraft, R. P., Sneden, C., Langer, G. E., & Prosser, C. F. 1992, AJ, 104, 645

Kraft, R. P., Sneden, C., Smith, G. H., Shetrone, M. D., Langer, G. E., & Pilachowski, C. A. 1997, AJ, 113, 279

Kurucz, R. 1993, Kurucz CD-ROM 13, ATLAS9 Stellar Atmosphere Programs and 2 km/s Grid (Cambridge: SAO)

Kurucz, R. L., Furenlid, I., & Brault, J. 1984, Solar Flux Atlas from 296 to 1300 nm (Sunspot: Natl. Solar Obs.)

Lambert, D. L., & Luck, R. E. 1976, Observatory, 96, 100

Lambert, D. L., Smith, V. V., Busso, M., Gallino, R., & Straniero, O. 1995, ApJ, 450, 302

Lattanzio, J., Karakas, A., Campbell, S., Elliott, L., & Chieffi, A. 2004, Mem. Soc. Astron. Italiana, 75, 322

Lucatello, S., Gratton, R., Cohen, J. G., Beers, T. C., Christlieb, N., Carretta, E., & Ramírez, S. 2003, AJ, 125, 875

Noguchi, K., et al. 2002, PASJ, 54, 855

Pasquini, L., Bonifacio, P., Molaro, P., François, P., Spite, F., Gratton, R. G., Carretta, E., & Wolff, B. 2005, A&A, 441, 549

Peterson, R. C. 1980, ApJ, 237, L87

Pilachowski, C. A., Sneden, C., Kraft, R. P., & Langer, G. E. 1996, AJ, 112, 545

Ramírez, S. V., & Cohen, J. G. 2003, AJ, 125, 224

Renzini, A., & Fusi Pecci, F. 1988, ARA&A, 26, 199

Shetrone, M. D. 1996a, AJ, 112, 1517

———. 1996b, AJ, 112, 2639

Sivarani, T., et al. 2004, A&A, 413, 1073

Smith, V. V., Cunha, K., Ivans, I. I., Lattanzio, J. C., Campbell, S., & Hinkle, K. H. 2005, ApJ, 633, 392

Smith, V. V., Suntzeff, N. B., Cunha, K., Gallino, R., Busso, M., Lambert, D. L., & Straniero, O. 2000, AJ, 119, 1239

Sneden, C. 1973, ApJ, 184, 839

Sneden, C., Cowan, J. J., Burris, D. L., & Truran, J. W. 1998, ApJ, 496, 235

Sneden, C., Cowan, J. J., Ivans, I. I., Fuller, G. M., Burles, S., Beers, T. C., & Lawler, J. E. 2000, ApJ, 533, L139

Sneden, C., Ivans, I. I., & Fulbright, J. P. 2004a, in Origin and Evolution of the Elements, ed. A. McWilliam & M. Rauch (Cambridge: Cambridge Univ. Press), 170

Sneden, C., Kraft, R. P., Guhathakurta, P., Peterson, R. C., & Fulbright, J. P. 2004b, AJ, 127, 2162

Suntzeff, N. B., & Smith, V. V. 1991, ApJ, 381, 160

Sweigart, A. V., & Mengel, J. G. 1979, ApJ, 229, 624

Tomkin, J., & Lambert, D. L. 1983, ApJ, 273, 722

———. 1999, ApJ, 523, 234

Travaglio, C., Gallino, R., Arnone, E., Cowan, J., Jordan, F., & Sneden, C. 2004, ApJ, 601, 864

Travaglio, C., Gallino, R., Busso, M., & Gratton, R. 2001, ApJ, 549, 346

van den Bergh, S. 1993, ApJ, 411, 178

Van Eck, S., Goriely, S., Jorissen, A., & Plez, B. 2001, Nature, 412, 793

———. 2003, A&A, 404, 291

Ventura, P., & D'Antona, F. 2005, A&A, 439, 1075

Yong, D., Grundahl, F., Lambert, D. L., Nissen, P. E., & Shetrone, M. D. 2003a, A&A, 402, 985 (Y03)

Yong, D., Grundahl, F., Nissen, P. E., Jensen, H. R., & Lambert, D. L. 2005, A&A, 438, 875 (Y05)

Yong, D., Lambert, D. L., & Ivans, I. I. 2003b, ApJ, 599, 1357